

A Momentum Filter for Atomic Gas

Wei Xiong, Xiaoji Zhou,* Xuguang Yue, Yueyang Zhai, and Xuzong Chen

School of Electronics Engineering & Computer Science, Peking University, Beijing 100871, China

(Dated: April 2, 2022)

We propose and demonstrate a momentum filter for atomic gas based on a designed Talbot-Lau interferometer. It consists of two identical optical standing-wave pulses separated by a delay equal to odd multiples of the half Talbot time. The one-dimensional momentum width along the long direction of a cigar-shaped condensate is rapidly and greatly purified to a minimum, which corresponds to the ground state energy of the confining trap in our experiment. We find good agreement between theoretical analysis and experimental results. The filter is also effective for non-condensed cold atoms and could be applied widely.

PACS numbers: 67.85.Hj, 67.85.Jk, 03.75.Kk

I. INTRODUCTION

Atomic sources with long coherence lengths, corresponding to a narrow momentum width, can be used to observe new physical phenomena and contribute to the improved precision measurement spectroscopy. Atomic clocks [1, 2] are for example greatly improved with narrower momentum width and so are the atomic interferometers [3, 4]. Large correlation lengths have been achieved with Bose-Einstein condensate [5, 6]. Many techniques have been used to actually reduce the momentum width of atomic gases. Some of them, such as the velocity-selective coherent population trapping (VSCPT) [7] and Raman filter [8], behave as momentum filters to select atoms with specific momenta and to discard the others. Other techniques benefit from the thought of filter to achieve lower temperature, such as evaporative cooling [9, 10] and Raman cooling [11].

In this paper, we report a momentum filter scheme by precisely discriminating the different momenta-related phase evolutions during a matter wave Talbot-Lau interference sequence. The Talbot effect was observed as a near-field diffraction with optical waves [12] and later observed with atoms [13–18]. In those works on the matter wave Talbot effect, the initial matter waves were approximated as a mono-energetic plane wave. In our work, the momentum distribution of a practical matter wave is considered. The effect of the momentum filter appears when an atomic gas is diffracted by a designed temporal Talbot-Lau interferometer with specific standing wave pulses and time intervals between the pulses. As a result, the interferometer generates different interference patterns for different initial momenta and behaves as a filter. When the filter is applied on condensates, we choose the intervals to be short enough (less than $11T_T/2$), so that the momentum filtering affects the scattering process more than the interaction energy induced by the

interaction between atoms. The redistributing and purifying effects of the filter are demonstrated in the experiments and also analyzed theoretically. With the filter, we are able to rapidly purify one dimensional momentum width of the atomic gas to a minimum, which is the momentum width of atoms in the ground state of the confining trap. Additionally, we discuss the influence of atomic interaction in the experiments above. The momentum filter is effective for both non-condensed cold atoms and condensate as shown in the experiment. We also discuss some possible applications of the filter.

This paper is organized as follows. In Sec. II, a physical model to interpret the momentum filter is presented. We derive a concise expression with Raman-Nath approximation [19] to reveal the physics of the filter, and then treat the standing wave as a one dimensional optical lattice for more precise description. We also discuss the effect of interaction between atoms for filters on condensates. Section III and IV present the effect of momentum redistribution and purification by the filter respectively. In Sec. V, the flexibility of the filter is demonstrated. Section VI contains discussion and conclusions.

II. PHYSICAL MODEL

Similarly to the optical Talbot-Lau effect, the temporal Talbot-Lau effect on matter wave behaves as shown in Fig. 1(a). Two standing wave (optical lattice) pulses with the same duration τ_0 and induced optical potential U_0 , behave as two gratings. The matter wave accumulates a phase shift during the time interval τ_f as what happens to a light wave along its optical path. The two effects both lead to the matter (optical) wave interference patterns.

Fig. 1(b) shows the mechanism of a band-pass momentum filter centered at zero momentum. The time interval τ_f is designed as odd multiples of the half Talbot time $T_T/2$, where the Talbot time T_T [18] is the minimum time for the matter wave front's reconstruction after the first pulse. An atomic gas with its momenta distributed around zero is diffracted into the components with mo-

*Electronic address: xjzhou@pku.edu.cn

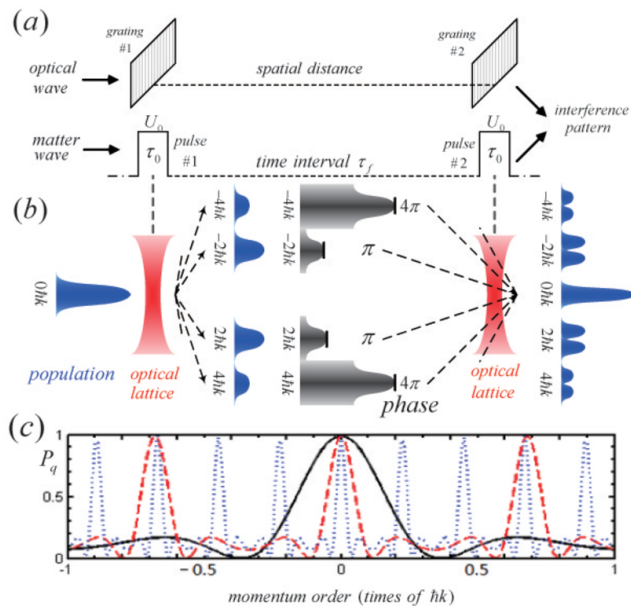


FIG. 1: (color online) The temporal Talbot-Lau effect on matter wave as a momentum filter. (a) The similarity between the optical and the matter wave Talbot-Lau effect. The input wave source is an optical (matter) wave. The two standing wave pulses behave as the two gratings. The phase of the light wave evolves along the space distance similarly as the matter wave during the time interval. (b) The scheme of the momentum filter. An atomic cloud with a momentum distribution around zero is scattered to be around momenta $\pm 2n\hbar k$ ($n = 0, 1, 2, \dots$) by the first pulse. During a time delay $T_T/2$, the atoms with momenta centered around $\pm 2n\hbar k$ acquire a phase shift around $n^2\pi$. After the second pulse, the atoms with the initial momenta closer to zero will be more probably scattered back into the initial state. (c) The relation between the probability P_q and its initial momentum q . The solid, dashed and dotted line correspond to the interval of $T_T/2$, $3T_T/2$ and $9T_T/2$.

momenta around $\pm 2n\hbar k$ ($n = 0, 1, 2, \dots$, the Planck constant \hbar , the wave vector of the light for the standing wave k) by the first pulse. With the interval $T_T/2$, the atoms with momenta $\pm 2n\hbar k$, which originate from the atoms with initial zero momentum, obtain the accurate phase evolution $n^2\pi$ (which can be simplified as $n\pi$ because n^2 and n have the same parity), and the second pulse entirely diffracts them back to their initial states. For the atoms with non-zero initial momenta, the larger the initial momentum is, the larger the phase deviation from $n^2\pi$ is and the more imperfect the recurrence will be, which results in a momentum filtering.

For a brief description of the filter, we consider the standing wave pulses to be short enough for the Raman-Nath approximation and obtain the probability of an atom with initial momentum q returning to the initial

state as:

$$P_q = \sum_{n=-\infty}^{+\infty} J_{-n}(\Omega\tau_0)J_n(\Omega\tau_0)e^{-iE_{n,q}\tau_f/\hbar}, \quad (1)$$

with the Bessel function of the first kind J_n , the two-photon Rabi frequency Ω [20], the kinetic energy $E_{n,q} = (2n\hbar k + q)^2/2M$ and the atomic mass M . While the interval is designed as $\tau_f = (2N + 1)T_T/2$, ($N = 0, 1, 2, \dots$), the atoms with initial zero momentum accumulate the phase as $E_{n,0}\tau_f/\hbar = n^2(2N + 1)\pi$, and the probability reaches the maximum as $P_{q=0} = 1$.

Afterwards, we apply the Bloch theorem for a more precise description of the scattering process as described in [21], where the standing wave is considered as an optical lattice and re-calculate the probability P_q as shown in Fig. 1(c). It can be seen from the figure that the momentum filter actually consists of a series of filters with different centers. The filter can be described as long as the width and position of each filter are definite. The $1/e$ width $2q_0$ of a single filter can be evaluated based on $P_{q_0} = 1/e$. Since the probability is principally influenced by the phase evolution during the interval, we introduce a phase shift index α , which satisfies $\alpha\pi = (E_{1,q_0} - E_{1,0})\tau_f/\hbar \approx 2kq_0\tau_f/M$, while $q_0 \ll 2\hbar k$ is easily satisfied. The index α indicates the phase deviation between the atoms with the momentum $2\hbar k$ and $2\hbar k + q_0$ during the interval. It reveals the relation between the interval and the width of a single filter as:

$$2q_0 \approx M\alpha\pi/k\tau_f \quad (2)$$

Since τ_f is equal to $(2N + 1)T_T/2$, the width is also of discrete values. As shown in Fig. 1(c), when the interval is increased, the width of the filter decreases and so does the distance δq between adjacent centers. This distance means that the atoms with an initial momentum difference δq will obtain the same interference pattern after the filter, since the phase deviation $(E_{n,q+\delta q} - E_{n,q})\tau_f/\hbar$ is integral multiple of 2π . According to our analysis, δq satisfies $\delta q = 2\hbar k/(2N + 1)$, which can also be drawn from the figure.

We analyze the momentum filter with single-atom model above, which works for non-condensed cold atoms. When the atomic source is a condensate, interaction between atoms needs to be considered. When condensates are scattered by one dimensional filter sequence, the interaction between atoms takes effect. The widths of light pulses (several μs generally) are much shorter than the characteristic time of interaction energy (magnitude as ms), so interaction during light pulses can be neglected. Atomic interaction can not be ignored so easily during intervals between light pulses, because intervals are possibly comparable with the characteristic time of the interaction shift. For a condensate in a harmonic trap exposed to a one-dimensional momentum filter, its interaction energy can be averaged in the plane perpendicular to the lattice direction and get a distribution along the lattice direction as $E_I = E_0(1 - z^2/R_z^2)$, with the interaction

energy maximum E_0 in lattice direction Z , the coordinate of lattice direction z and the Thomas-Fermi radius R_Z of the condensate along this direction.

According to the Gross-Pitaevskii equation, the phase of $2\hbar k$ component after the first lattice pulse evolves as $e^{-i(E_k+V+E_I)\tau_f/\hbar}$, with the kinetic energy E_k along Z direction and magnetic trap V . The frequency of the magnetic trap along Z direction is only 20Hz , so it can be neglected, compared with the other two components. The kinetic energy is related to the Talbot time as $E_k/(2\pi\hbar) = 1/T_T$. For the initial momentum q corresponding to a momentum width introduced by momentum filter, the rate of its induced phase shift is $(2\hbar k + q)^2 - (2\hbar k)^2/2M\hbar \approx 2\hbar k \times q/M\hbar$.

On the other hand, for interaction between atoms along the Z direction, the average of interaction energy is 80% of the maximum. The rate of the phase shift induced by interaction can be approximated as $E_0/5\hbar$. If the rate of the phase shift induced by the initial momentum is larger, i. e. $2\hbar k \times q/M > E_0/5$, momentum filter plays a main role in the scattering process. Otherwise, interaction energy plays a major role.

In our experiment, the Talbot time is $T_T = 76\mu\text{s}$, and the initial momentum q leads to a rate of phase shift as $q/\hbar k \times 13.16\text{kHz}$. The interaction energy is about 1.5kHz at the center of the atomic cloud in our experiment and its distribution along Z direction after average is $1\text{kHz} \times (1 - z^2/R_Z^2)$. The rate of phase shift induced by atomic interaction is about 200Hz in our experiment. While interval increases, the corresponding momentum width decreases, and the phase evolution rate relevant to the momentum width also decreases. On the other hand, the phase evolution rate induced by interaction is independent of the interval, so these two rates can be equal with a certain interval. When the rates introduced by initial momentum and interaction are equal, the interval is $6T_T$ and it means that the effect of momentum filter plays bigger role than the interaction when the interval is shorter than that, and things are opposite when the interval is longer. The interaction induced phase shift is position dependent and the interaction energy will accelerate the phase evolution of atoms around the center of atomic cloud. The filtered fraction results of both momentum filter and interaction energy effects. As a result, we demonstrate the momentum filter mainly within the regime, where intervals are less than $6T_T$.

III. MOMENTUM REDISTRIBUTION

We performed the experiments on a ^{87}Rb Bose-Einstein condensate (BEC) system [22, 23]. After pre-cooling, a cigar shaped ^{87}Rb condensate of 1×10^5 atoms in $5^2S_{1/2} |F=2, M_F=2\rangle$ state was achieved by radio frequency (RF) cooling in the a harmonic magnetic trap (MT), with 20Hz axial frequency and 220Hz radial frequency. The initial atomic gas is prepared as a condensate without observed non-condensed cold atoms. A one

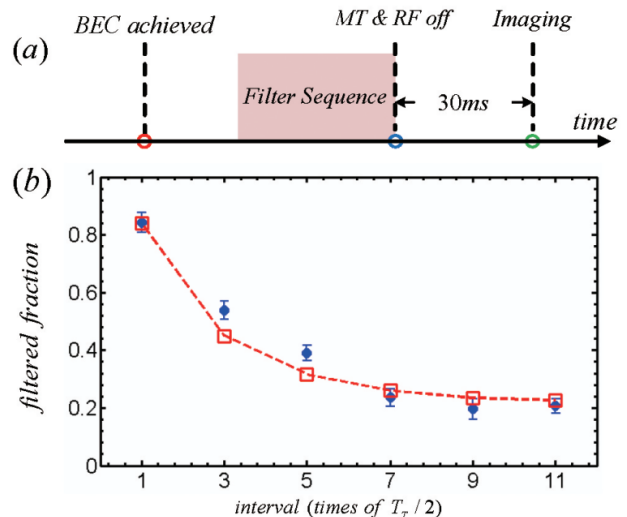


FIG. 2: (color online) Redistributing effect of the momentum filter. (a) Sequence of the experiment. (b) The ratio of the filtered atoms (N_0) over the total number of the atoms (N_A) versus the interval τ_f . The round solid dots are the experimental results and the hollow square dots are the theoretical analysis, considering that the effect of atomic gases' practical temperature and the momentum expansion induced by s wave scattering are equivalent to an initial momentum width $0.1\hbar k$.

dimensional designed far-red-detuned (the wavelength is 852nm) standing wave pulse sequence was applied onto the condensate along the axial direction. The lattice depth is $80E_R$, which is calibrated by Kapitza-Dirac scattering experimentally. In the experiments, we choose the width of a single pulse to be $3\mu\text{s}$, so that the first pulse is able to couple most of the atoms (about 60%) to the momenta $\pm 2\hbar k$, some atoms are populated around $\pm 4\hbar k$ (about 36%), others are around $0\hbar k$ and other momenta. The second pulse is the same as the first one. In our experiment, the Talbot time is $76\mu\text{s}$ and the index α is about 0.20. According to our calculation, the influences from momentum filter and atomic interaction are equal when the interval is $6T_T$, so we choose the interval from $T_T/2$ to $11T_T/2$ in experiments, where momentum filter plays bigger role.

We demonstrate the redistributing effect of our momentum filter by turning off the RF field and the magnetic trap simultaneously, after sending the pulse sequence. The time-of-flight (TOF) signal of the atoms is obtained after 30ms free fall (see Fig. 2(a)). As the interval increases, the bandwidth of the filter decreases and the relative population of the atoms returning to their initial states also decreases as shown in Fig. 2(b). For the non-condensed-cold-atom background of the cloud, its momentum distribution is classically Gaussian. However, for the condensate, when its momentum can not be neglected, Thomas-Fermi approximation is no longer valid and it is reasonable that its momentum distribution is analogous to Gaussian profile. Therefore, we describe

condensate's momentum distribution approximatively as ce^{-q^2/Δ^2} (the normalization coefficient c , the momentum q and the $1/e$ width 2Δ). In this way, we calculate the relative population (square hollow dots in the figure) of the filtered atoms, compare the calculation with the experimental results (round solid dots) and find that the calculation generally pictures the trend of experimental results. The decrease of filter bandwidth, derived from Eq. (2) as $\delta = 4\alpha\hbar k/(2N+1)(2N+3) \approx \alpha\hbar k/N^2$, shrinks rapidly as a function of N . As a result, the number of the filtered atoms changes more and more slowly while the interval τ_f increases by units of T_T in Fig. 2(b).

For the theoretical curve (see square hollow dots in Fig. 2(b)), atomic gases to be filtered are not pure condensates with zero temperature and s wave scattering [24] also introduces momentum dispersion during the recoil after the first pulse. We approximate these two effects as an average initial momentum width $0.1\hbar k$ [21]. When the intervals are short, the simulated filtered fractions are slightly higher than experimental ones, because the effective initial momentum widths are lower than $0.1\hbar k$. While the intervals get longer, the effective initial momentum widths are higher, so the filtered fractions are lower.

There are still some deviations between the calculation and the experiment, although the experimental results are normalized to minimize the uncertainty of the initial atom number. One of the possible reasons may be the assumed purity of the condensate in the theory. A practical condensate is always surrounded by a cloud of non-condensed cold atoms with much wider momentum width. The non-condensed cold atoms contribute little to the filtered component, but much more to the total atom number. As a result, the fluctuation of the non-condensed cold atom number leads to the deviation in our experiment with respect to theory.

In the experiment about momentum redistribution by a pulse sequence, when the interval τ_f is $17T_T/2$, we observed two holes at the position of the momenta $\pm 2\hbar k$ in TOF signal as shown in Fig. 3(c). With this interval, the rate of phase shift induced by momentum corresponding to the width of the filter is 141Hz and that induced by interaction is still 200Hz , so that the two holes originate from both position selection by atomic interaction and momentum filtering. We numerically simulated the process with the only difference that the initial condensate is with (see Fig. 3(b)) or without (see Fig. 3(a)) atomic interaction. The two simulations clearly show the effect introduced by atomic interaction.

As shown in Fig. 3(a), for condensate without atomic interaction, many peaks appear in the component around $0\hbar k$, and each peak corresponds to a certain center of the filter, because the absence of atomic interaction leads to little expansion in TOF signal and none of other redistributing effects. Consequently, only the momenta parts produced by the filter can be seen and the valleys in the $\pm 2\hbar k$ components also illustrate that. In Fig. 3(b), for condensate with atomic interaction, only one peak

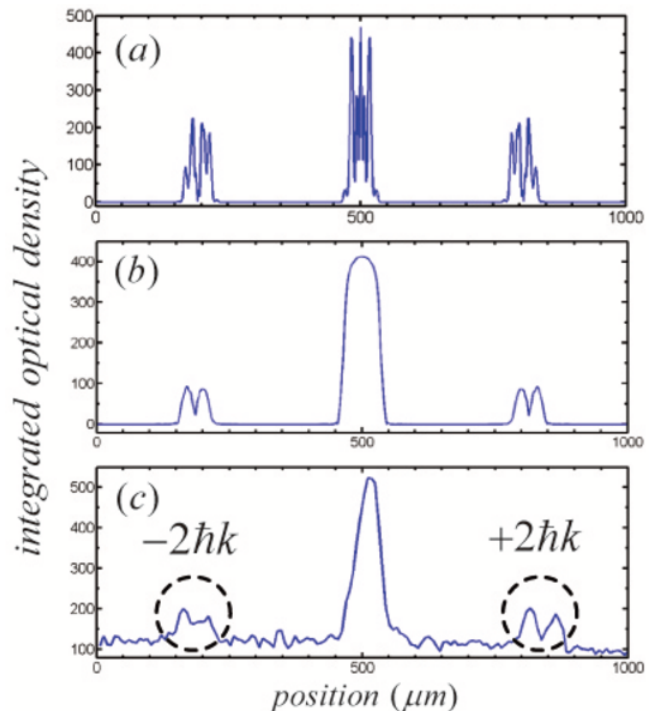


FIG. 3: (color online) Redistribution introduced by both momentum filter and atomic interaction. (a) A numerical simulation of TOF signal considering momentum filter without interaction. (b) A numerical simulation of TOF signal including momentum filter and atomic interaction. (c) A TOF signal obtained in our experiment. Two holes around $\pm 2\hbar k$ components can be observed.

emerges around $0\hbar k$, and it is because that interaction leads to expansion and blur the peaks in TOF signal. However, two valleys arise around $\pm 2\hbar k$ separately. They are wider than the ones in condensate without interaction and obviously come from phase gradient introduced by atomic interaction, except for the filter. We numerically analyzed the process and found that the result is generally consistent with the experimental result. The holes in Fig. 3(c) are even larger, and the reasons may be dispersion induced by s -wave scattering, deviation from imaging system and so forth.

IV. MOMENTUM PURIFICATION

To observe the momentum purifying effect of the filter, we manage to keep the filtered component in the magnetic trap and discard the others. As described in Fig. 4(a), the magnetic trap and the RF field are maintained for 12.5ms (a quarter of the period of the magnetic trap along the axial direction) after the filter sequence. The atoms with higher momentum will move away to higher potential positions of the magnetic trap and be driven out by the RF field. On the other hand, the remaining atomic gas kept in the trap evolves dur-

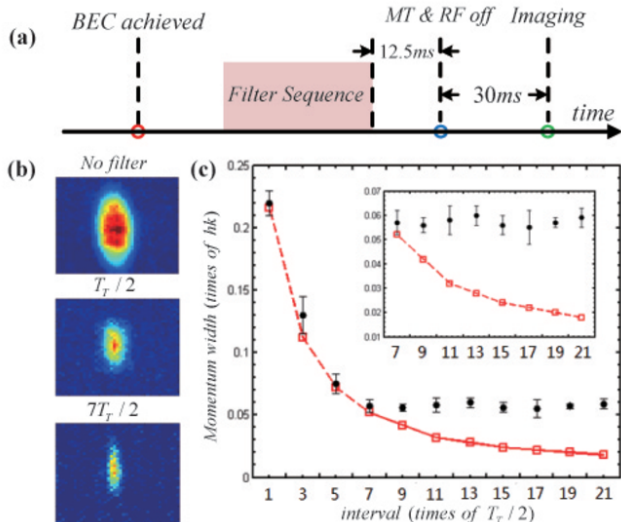


FIG. 4: (color online) Purification effect of the momentum filter. (a) Time sequence for momentum narrowing. (b) TOF signals demonstrating one dimensional momentum narrowing. The figures from top to bottom show a condensate without filtering, a condensate modified by a filter with interval $T_T/2$ and a condensate purified by a filter with interval $7T_T/2$ respectively. (c) Momentum width versus the interval of the filter. The hollow square dots are theoretical results and the solid round dots are experimental results.

ing this time. The $1/e$ width $Z(0)$ of the atomic gas at the moment of being released from the magnetic trap can be calculated based on the wave function of the condensate after the filter. The evolution of the atomic gas can be figured out according to the time-dependent Gross-Pitaevskii equation. We are able to evaluate the momentum width after the free falling time t from the TOF signal by working out the ballistic expansion equation $Z^2(t) = Z^2(0) + (2q_0/M)^2 t^2$, with the size $Z(t)$ of the cloud along the lattice direction.

The TOF signal in Fig. 4(b) demonstrates the one dimensional momentum purification with increased interval. The reduction of the atomic cloud size along the lattice direction from the TOF signals pictures clearly the effect of the momentum purification. The figures from top to bottom show a condensate without filtering, a condensate modified by a filter with interval $T_T/2$, a condensate purified by a filter with interval $7T_T/2$ respectively. The atomic size along the lattice direction in the figure at the bottom is the narrowest one we can get in the experiment.

The atomic cloud with the narrowest size we obtained in experiment was not in the Q2 ThomasCFermi regime. The atomic cloud contained about 2×10^4 atoms. If it reached thermal equilibrium and were in the Thomas-Fermi regime, its initial size in the trap along Z direction would be $2R_Z = (2\mu_N/m\omega_Z^2)^{1/2} \approx 52\mu m$ (μ_N is the chemical potential related to s-wave scattering length a , atomic number N_0 and geometrical frequency of the mag-

netic trap ω as $\mu_N = (15N_0\hbar^2 a/(4\sqrt{2}M))^{2/5}(M\omega^2)^{3/5}$). After 30ms expansion, the size of atomic cloud would reach $60\mu m$, which is much larger than $28\mu m$ as observed in experiment. As a result, the size of atomic cloud's shrinking mainly depends on momentum purifying, but not the decrease of atomic number.

The achieved one dimensional momentum width by the filters with increased interval is shown in Fig. 4(c). The momentum width predicted by the calculation (square hollow dots) goes along with the experimental results (round solid dots) well until the interval of the filter exceeded $7T_T/2$, which corresponds to the expected width $0.052\hbar k$. When the atomic gas is abruptly released from the magnetic trap, its potential energy vanishes but the kinetic half remains, so the average kinetic energy of the atomic gas in free space can not get lower than that of the ground state of the confining trap. The frequency $20Hz$ of the axial magnetic trap corresponds to the momentum width $0.056\hbar k$ as $(0.028\hbar k)^2/M = \hbar \times 20Hz/4$ and this is the reason why the momentum width of the atomic gas keeps this value, although a filter with longer interval is in principle able to further purify the momentum width.

We can still observe narrow size of atomic gas, even with very long interval (up to $21T_T/2$). The reason is as follows. Although interaction is present during the process, it only leads to an imperfection of the momentum filter as it decreases the probability of atoms with initial momentum around zero to return to their original states. The momentum filter still purifies the momentum width as anticipated. The interaction energy is position dependent, not momentum dependent. It affects the population of the momentum-filtered component, but hardly the momentum width. On the other hand, the ground state energy of our magnetic trap is a stronger constraint to the momentum width of the released atomic gas. We observe the narrowest kinetic energy dispersion of the released atomic gas corresponds to the ground state energy of the trap, achieved for a filter using a $7T_T/2$ interval. When intervals are longer than that, neither the effect of the momentum filter nor that of the interaction energy can be observed on the momentum widths. As a result, we can still observe atomic clouds shrinking to the narrowest size with very long intervals in our experiments.

V. FLEXIBILITY OF THE FILTER

We show in this section that the filter can be applied flexibly, as it can be used for both non-condensed cold atoms and condensate. Several filters can be combined to a new one and the center of a filter may also be adjusted.

The effectiveness of the filter for different kinds of atomic gases is demonstrated in Fig. 5. The effect of a filter for non-condensed cold atoms is shown in Fig. 5(a) with the interval $T_T/2$ and that of a filter with the interval $5T_T/2$ on a mixture of condensate and non-condensed cold atoms is shown in Fig. 5(b). The re-shaping of the momentum distribution can be obviously observed from

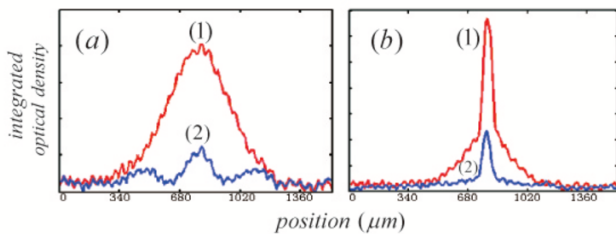


FIG. 5: (color online) TOF signals showing the filtering on two kinds of atomic gases. Curve (1) is the initial atomic gas and curve (2) is the atomic gas after the filter. (a) A cloud of non-condensed cold atoms with temperature $513nK$ modified by a filter with the interval $T_T/2$. (b) A mixture of condensate and non-condensed cold atoms with temperature $346nK$ modified by a filter with the interval $5T_T/2$.

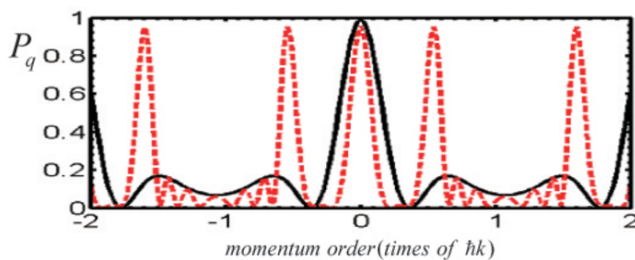


FIG. 6: (color online) Comparison between single filter and two combined filters. The solid curve is the probability of recurrence for the single filter with interval $T_T/2$, the dashed one is that for a combination of two same filters with interval $T_T/2$ linked by a $T_T/2$ time delay.

the TOF signal. Actually, there is no restriction with respect to the choice of the initial atomic cloud for the filter, but the parameters of the filter still need to be optimized for the observation of the filter effect.

Combination of single filters is a possible choice for achieving narrower width. The probabilities of recurrence after a single filter with the interval $T_T/2$ and two combined same filters are compared in Fig. 6. The probability of the combined one is not simply the production of two single filters, because for the second filter sequence, the filtered component is the superposition of the states with a series of different phases instead of a pure state with the same phase as the initial state; additionally, the components with the momenta $\pm 2n\hbar k$ still remain in the atomic gas and play a role in the interference of the second filter sequence. However, the combination still behaves as a filter with a narrower momentum width.

The center of the momentum filter is not confined to be only zero, such as some value q_c , we can design the filter with time constant τ_f as $E_{n,q_c}\tau_f/\hbar = (2N+1)\pi$ ($N = 0, 1, 2, \dots$) with similar bandwidth. For instance, if the intervals are $2T_t/2, 4T_t/2, \dots$, the minimum centers of the corresponding filters will be $\hbar k/2, \hbar k/4, \dots$

VI. DISCUSSION AND CONCLUSIONS

This momentum filter actually utilizes the interference among all the momentum states generated by the first lattice pulse to form a momentum filter. Although the $|\pm 2\hbar k\rangle$ and $|\pm 4\hbar k\rangle$ states overwhelm the others after the first pulse, the filter will be less functional if the other momentum states are neglected, let alone the $|\pm 4\hbar k\rangle$ states also being canceled. The consequence of ignoring higher orders' momentum states is that the filter will miss some zero momentum atoms and collect more non-zero components and the momentum distribution will be broadened.

The momentum width achieved by the filter may be limited by the following factors. The first one is the initial momentum width of the atomic gas. The initial momentum distribution can cover several centers of the filter. Although the increased interval can reduce the bandwidth, the non-zero centers will weaken the purifying of the momentum. The second one is the relative line width γ of the laser of filter, since the interval can not increase for failure of discriminating the phase shift due to the line width, which means $((2\hbar k(1+\gamma))^2 - (2\hbar k)^2)\tau_f/2M\hbar \leq \alpha\pi$. The third one is the de-coherence time. The filter is a process of interference, so there will be no filter if the quantum states de-coherent during the interval of the filter.

In our experiment, the narrowest momentum width achieved with this filter is limited by the confining trap. If the confinement of the trap is weaker, the momentum filter will be able to generate narrower momentum widths. The experiments can be extended to three dimensions, since three dimensional optical lattice is widely used at present. The three dimensional filter could be a tool for rapidly cooling atomic gases.

This filter is not a repetitive demonstration of Talbot-Lau interferometer, since the matter wave we dealt with is distributed in momentum space, not a simple plain wave. As a result, the momentum selecting effect comes out from the interferometer. Briefly compared with other momentum filters, our filter is simple and robust.

Firstly, requirements on lasers are different in our filter and other velocity selection methods. Our filter consists of optical lattice pulse sequences, which are easily designed and controlled. The lattice laser is so far detuned from atomic resonance that the filter can work well without laser frequency lock. This means a good many kinds of atoms and molecules can be momentum purified by lasers with a very wide range of frequencies, through our method. By comparison, optical setups for Raman filter and VSCPT are more complicated. For Raman filter, in order to preserve the atoms with specific momenta and to blow off the others, at least two different frequency laser beams are needed. Otherwise, the selected atoms have to be charged a momentum $2\hbar k$. Furthermore, laser frequencies have to be locked to make sure that Rabi frequency matches the pulse duration.

Secondly, our filter preserves both the internal and external states of selected atoms. It hardly changes the

momenta or the internal states of the selected atoms, and simultaneously charges other atoms with momenta $\pm 2\hbar k$, $\pm 4\hbar k$ and so on. Consequently, our filter can work solo and cooperate with other techniques smoothly, such as evaporative cooling. For Raman filter, if the internal states of filtered atoms need to be preserved, they have to be charged with a momentum $2\hbar k$; if the momenta of the selected atoms are preserved, they have to be pumped into another internal state. Otherwise, the atoms both preserving momenta and internal states are difficult to distinguish from others.

Thirdly, our filter is robust for atoms being in the dark during most of the filter process. When lattice is on, lasers in our filter can work well with very large detuning (taking ^{87}Rb for example, its $D1$ line resonates at 795nm , our lattice light works at 852nm) and very short pulses (in our experiment, pulse duration can be as short as $1\mu\text{s}$ while lattice depth reaches $120E_R$); during the rest of the filter process (in our experiment, the interval between two lattice pulses is about $300\mu\text{s}$ to achieve the momentum width $0.056\hbar k$), atoms stay in the dark. As a result, the filter can hardly be disturbed by most of the perturbations and drifts on lattices frequency, phase and intensity, such as vibration noise on optical lattice mirror, because these noise frequencies are mostly below 1MHz . In contrast, in order to achieve similar momentum width, the pulse duration in Raman filter is usually about 2ms , and noises with frequency higher than 500Hz will be received by the system. Dark states in VSCPT are much more fragile. Hence, our filter is of great potential to achieve ultra-narrow momentum width because a

lot of noises are shielded.

In conclusion, we apply a designed temporal matter wave Talbot-Lau interferometer for realizing a momentum filter, which can keep the atoms with lower momenta in their initial states and drive the others to states with higher momenta. This kind of momentum filter makes use of the momentum-state interference to discriminate between momenta and hardly depends on the transition between the atomic internal states. With such filter, we manage to prepare an atomic cloud with $0.056\hbar k$ momentum width within $300\mu\text{s}$. We consider the interaction between atoms for condensate during the filter process, and find that it affects the redistribution of atomic gas, but hardly momentum purifying. We show that it is an effective method for rapidly compressing the momentum width of an atomic gas, and systematically discuss the specifications of the filter. It may be of great potential for achieving ultra low temperatures.

Acknowledgement

We appreciate H. W. Xiong, G. V. Shlyapnikov, G. J. Dong, L. B. Fu, B. Wu and H. zhai for stimulating discussions. We thank Thibault Vogt for critical reading of our paper. This work is supported by the National Fundamental Research Program of China under Grant No. 2011CB921501, the National Natural Science Foundation of China under Grant No. 61027016, No.61078026 and No.10934010.

-
- [1] Mark A. Kasevich *et al.*, Phys. Rev. Lett. **63**, 612(1989).
 - [2] R. Wynands *et al.*, Metrologia **42**, 64(2005).
 - [3] Alexander D. Cronin *et al.*, Rev. Mod. Phys. **81**, 1051 (2009).
 - [4] J. B. Fixler *et al.*, Science **315**, 74 (2007).
 - [5] M. H. Anderson *et al.*, Science **269**, 198 (1995).
 - [6] K. B. Davis *et al.*, Phys. Rev. Lett. **75**, 3969(1995).
 - [7] A. Aspect *et al.*, Phys. Rev. Lett. **61**, 826(1988).
 - [8] M. Kasevich *et al.*, Phys. Rev. Lett. **66**, 2297(1991).
 - [9] Wolfgang Ketterle *et al.*, Advances in atomic molecular and optical physics **37**, 181-236(1996).
 - [10] K. B. Davis *et al.*, Phys. Rev. Lett. **74**, 5202(1995).
 - [11] M. Kasevich and S. Chu Phys. Rev. Lett. **69**, 1741(1992).
 - [12] William B. Case *et al.*, Optics Express **17**, 23 (2009)
 - [13] Michael S. Chapman *et al.*, Phys. Rev. A **51**, 1 (1995).
 - [14] J. F. Clauser and M. W. Reinsch Appl. Phys. B **54**, 380 (1992).
 - [15] S. Nowak *et al.*, Opt. Lett. **22**, 1430 (1997).
 - [16] J. F. Clauser *et al.*, Phys. Rev. A **49**, R2213 (1994).
 - [17] O. Carnal *et al.*, Phys. Rev. A **51**, 3079 (1995).
 - [18] L. Deng *et al.*, Phys. Rev. Lett. **83**, 5407(1999).
 - [19] M. Edwards *et al.*, Phys. Rev. A **82**, 063613 (2010).
 - [20] A. F. Linskens *et al.*, Phys. Rev. A **54**, 6 (1996).
 - [21] W. Xiong *et al.*, Phys. Rev. A **84**, 043616 (2011).
 - [22] X. Zhou *et al.*, Phys. Rev. A **81**, 013615 (2010).
 - [23] B. Lu *et al.*, Phys. Rev. A **83**, 051608(R) (2011).
 - [24] Y. B. Band *et al.*, Phys. Rev. Lett. **84**, 5462(2000).